別紙4

雑誌

発表者氏名	論文タイトル名	発表誌名	巻名	ページ	出版年
Morita H, Kaneko H, Ohnishi H, Kato Z, Kondo N	Antigen-specific immune response to endotoxin-free recombinant p34.	Allergy			in press
Kaneko H, Fukao T, Kasahara K, Yamada Y, Kondo N	Augmented cell death with human and mouse Bloom syndrome helicase deficiency	Mol Med Rep			in press
Kaneko H, Teramoto T, Kondo M, Morita H, Ohnishi H, Orii K, Matsui E, Kondo N	Efficacy of the slow dose-up method for specific oral tolerance induction for children in cow's milk allergy: Comparison with previous reported protocols.	Journal of Investigational Allergology and Clinical Immunology	20	538-539	2010
Matsui E, Shinoda S, Fukutomi O, Kaneko H, Fukao T, Kondo N	Relationship between the benefits of suplatast tosilate, a Th2 cytokine inhibitor, and gene polymorphisms in children with bronchial asthma.	Experimental and therapeutic medicine	1	977-982	2010
Kondo N, Matsui E, Nishimura A, Kaneko H	Pharmacogenetics of asthma in children.	Allergy Asthma Immunol Res	2	14-19	2010
Ozeki M, Funato M, Teramoto T, Ohe N, Asano T, Kaneko H, Fukao T, Kondo N	Reversible cerebrospinal fluid edema and porencephalic cyst, a rare complication of ventricular catheter.	J Clin Neurosci	17	658-661	2010
Ozeki M, Kunishima S, Kasahara K, Funato M, Teramoto T, Kaneko H, Fukao T, Kondo N.	A family having type 2B von Willebrand disease with an R1306W mutation: Severe thrombocytopenia leads to the normalization of high molecular weight multimers.	Thromb Res	125	e17-22	2010
Fukao T, Horikawa R,Naiki Y, Tanaka T, Takayanagi M, Yamaguchi S, Kondo N	A Novel Mutation (c.951C>T) in an Exonic Splicing Enhancer Results in Exon 10 Skipping in the Human Mitochondrial Acetoacetyl-CoA Thiolase Gene	Mol Genet Metab	100	339-344	2010
Fukao T, Ishii T, Amano N, Kursula P, Takayanagi M, Murase K, Sakaguchi N, Kondo N, Hasegawa T.	A neonatal onset succinyl-CoA: 3-ketoacid CoA transferase (SCOT)-deficient patient with T435N and c.658-666dupAACGTGATT p.N220_I222dup mutations in the OXCT1 gene.	J Inherit Metab Dis	33	636	2010
Hori T, Fukao T, Kobayashi H, Teramoto T, Takayanagi M, Hasegawa Y, Yasuno T, Yamaguchi S, Kondo N.	Carnitine palmitoyltransferase 2 deficiency: The time-course of blood and urinary acylcarnitine levels during initial L-carnitine supplementation.	Tohoku J Exp Med	221	191-195	2010
Fukao T, Sass JO, Kursula P, Thimm E, Wendel U, Ficicioglu C, Monastiri K, Guffon N, Varic I, Zabot M-T, Kondo N.	Clinical and molecular characterization of five patients with Succinyl-CoA:3-ketoacid CoA transferase (SCOT) deficiency	Biochimica Biophysica Acta Molecular Basis of Disease			In press
Tsunoda S, Yachie A, Wakasugi H, Matsushita K, Yamaguchi Y, Kawano M.	A case of IgG4-positive multiorgan lymphoproliferative syndrome: dramatic perturbations of the CD8-positive T-cell repertoire in peripheral blood.	Scand. J. Rheumatol.	39	520-530	2010
Toga A, Wada T, Sakakibara Y, Mase S, Araki R, Tone Y, Toma T, Kurokawa T,Yanagisawa R, Tamura K,Nishida N, Taneichi H, Kanegane H, Yachie A	Clinical significance of cloned expansion and CD5 down-regulation in Epstein-Barr Virus (EBV)-infected CD8+ T lymphocytes in EBV-associated hemophagocytic lymphohistiocytosis.	J. Infect. Dis.	201	1923-1932	2010

別紙4

Asai E, Wada T, Sakakibara Y, Toga A, Toma T, Shimizu T, Nampoothiri S, Imai K, Nonoyama S, Morio T, Muramatsu H, Kamachi Y, Ohara O, Yachie A.	Analysis of mutations and recombination activity in RAG-deficient patients.	Clin. Immunol.	138	172-177	2011
Shinya Adachi, Heima Sakaguchi, Takashi Kuwahara, Yasushi Uchida, Toshiyuki Fukao and Naomi Kondo	High Regression Rate of Coronary Aneurysms Developed in Patients with Immune Globulin-Resistant Kawasaki Disease	Tohoku J Exp Med	220	285-290	2010
Yasushi Uchida, Hideyuki Morita, Shinya Adachi, Tsutomu Asano, Toshiaki Taga and Naomi Kondo	Bacterial meningitis of neonate due to Lactococcus lactis	Pediatr Int	in press		
Takahashi K, Oka A, Mizuguchi M, Saitoh M, Takita J, Sato A, Mimaki M, Kato M, Ogawa S, Igarashi T	Interstitial deletion of 13q14.13-q32.3 presenting with Arima syndrome and bilateral retinoblastoma	Brain Dev			Aug.19, 2010
Minobe K, Ono R, Matsumine A, Shibata-Minoshima F, Izawa K, Oki T, Kitaura J, Iino T, Takita J, Iwamoto S, Hori H, Komada Y, Uchida A, Hayashi Y, Kitamura T, Nosaka T.	Expression of ADAMTS4 in Ewing's sarcoma	Int J Oncol	37	569-581	2010
Okazaki K, Unemoto J, Kondo M, Kusaka T, Kozawa K, Yoshizumi M, Shimada A, Takita J, Kaneko T, Hama T, Kimura H.	Sustained cytokinemia and chemokinemia concomitant with juvenile myelomonocytic leukemia in an infant with Noonan syndrome	Leuk Res	34	e226-228	2010
Tsuchida M, Ohara A, Manabe A, Takita J (Collaborator 83); Tokyo Children's Cancer Study Group	Long-term results of Tokyo Children's Cancer Study Group trials for childhood acute lymphoblastic leukemia, 1984-1999	Leukemia	24	383-396	2010
Tumurkhuu M, Saitoh M, Sato A, Takahashi K, Mimaki M, Takita J, Takeshita K, Hama T, Oka A, Mizuguchi M	Comprehensive genetic analysis of overlapping syndromes of RAS/RAF/MEK/ERK pathway	Pediatr Int	52	557-562	2010
Okamoto T, Koh K, Takita J, Ida K	Voriconazole-micafungin combination therapy for acute lymphoblastic leukem	Pediatr Int	52	137-141	2010
滝田順子	ゲノムアレイと小児固形腫瘍-がんゲノミクスに基づいた標的分子の同定	日本小児がん学会雑誌	47	248-251	2010
滝田順子, 小川誠司	小児固形腫瘍における網羅的ゲノム解析と標的分子の同定	細胞工学	29	706-710	2010
Akahane K, Inukai T, Inaba T, Kurosawa H, Look AT, Kiyokawa N, Fujimoto J, Goto H, Endo M, Zhang X, Hirose K, Kuroda I, Honna H, Kagami K, Goi K, Nakazawa S, Sugita K.	Specific induction of CD33 expression by E2A-HLF: the first evidence for aberrant myeloid antigen expression in ALL by a fusion transcription factor.	Leukemia.	24(4):	865-9.	2010
Onda K, Iijima K, Katagiri YU, Okita H, Saito M, Shimizu T, Kiyokawa N.	Differential effects of BAFF on B cell precursor acute lymphoblastic leukemia and Burkitt lymphoma.	Int J Hematol.	91(5)	808-19.	2010
Hirose K, Inukai T, Kikuchi J, Furukawa Y, Ikawa T, Kawamoto H, Oram SH, Göttgens B, Kiyokawa N, Miyagawa Y, Okita H, Akahane K, Zhang X, Kuroda I, Honna H, Kagami K, Goi K, Kurosawa H, Look AT, Matsui H, Inaba T, Sugita K.	Aberrant induction of LMO2 by the E2A-HLF chimeric transcription factor and its implication in leukemogenesis of B-precursor ALL with t(17;19).	Blood.	116(6)	962-70.	2010
Miyagawa Y, Okita H, Hiroyama M, Sakamoto R, Kobayashi M, Nakajima H, Katagiri YU, Fujimoto J, Hata JI, Umezawa A, Kiyokawa N.	A microfabricated scaffold induces the spheroid formation of human bone marrow-derived mesenchymal progenitor cells and promotes efficient adipogenic differentiation.	Tissue Eng Part A	(in press)		

別紙4

Sasaki N, Hirano T, Kobayashi K, Toyoda M, Miyakawa Y, Okita H, Kiyokawa N, Akutsu H, Umezawa A, Nishihara S.	Chemical inhibition of sulfation accelerates neural differentiation of mouse embryonic stem cells and human induced pluripotent stem cells.	Biochem Biophys Res Commun.	401(3)	480-6.	2010
Kaneko T, Okita H, Nakajima H, Iijima K, Ogasawara N, Miyagawa Y, Katagiri YU, Nakagawa A, Kiyokawa N, Sato T, Fujimoto J.	Neuroblastoma cells can be classified according to distinctive glycosphingolipid expression profiles identified by liquid chromatography-tandem mass spectrometry.	Int J Oncol.	37(5)	:1279-88.	2010
Nishino K, Toyoda M, Yamazaki-Inoue M, Makino H, Fukawatase Y, Chikazawa E, Takahashi Y, Miyagawa Y, Okita H, Kiyokawa N, Akutsu H, Umezawa A.	Defining hypo-methylated regions of stem cell-specific promoters inhuman iPS cells derived from extra-embryonic amnions and lung fibroblasts	PLoS One.	27;5(9)	:e13017.	2010
Inamura M, Kawabata K, Takayama K, Tashiro K, Sakurai F, Katayama K, Toyoda M, Akutsu H, Miyagawa Y, Okita H, Kiyokawa N, Umezawa A, Hayakawa T, Furue MK, Mizuguchi H.	Efficient generation of hepatoblasts from human ES cells and iPS cells by transient overexpression of homeobox gene HEX.	Mol. Ther.	(in press)		
Ogasawara N, Katagiri YU, KiyokawaN, Kaneko T, Sato B, Nakajima H, Miyagawa Y, Kushi Y, Ishida H, Kiso M, Okita H, Sato T, Fujimoto J.	Accelerated biosynthesis of neolactoseries-glycosphingolipids in differentiated mouse embryonal carcinoma F9 cells detected by using dodecyl N-acetylglucosaminide as a saccharide primer.	J Biochem	(in press)		
清河信敬, 恩田恵子, 高野邦彦, 藤本純一郎, 真部淳, 康勝好, 小原明, 林泰秀, 花田良二, 土田昌宏	9 colorフローサイトメトリーによる小児白血病のマーカー解析	Cytometry Research	20(2)	27-34.	2010
Flow cytometric analysis of de novo acute myeloid leukemia in childhood: report from the Japanese Pediatric Leukemia/Lymphoma Study Group.	Flow cytometric analysis of de novo acute myeloid leukemia in childhood: report from the Japanese Pediatric Leukemia/Lymphoma Study Group.	Int J Hematol.			in press

IV. 研究成果の刊行物・別刷

Molecular Medicine Report in press

Augmented cell death with human and mouse Bloom syndrome helicase deficiency

Hideo Kaneko[1], Fukao Toshiyuki[1], Kimiko Kasahara[1], Taketo Yamada[2] and Naomi Kondo[1]

1) Department of Pediatrics, Graduate School of Medicine, Gifu University,
1-1 Yanagido, Gifu 501-1194, Japan
2) Department of Pathology. Keio University

Corresponding author: Hideo Kaneko
Department of Pediatrics, Graduate School of Medicine, Gifu University, 1-1 Yanagido, Gifu 501-1194, Japan
Tel: +81-58-230-6386
Fax: +81-58-230-6387
E-mail hideo@gifu-u.ac.jp

Abstract

Bloom syndrome (BS) is a rare autosomal genetic disorder characterized by lupus like erythematous telangiectasias of the face, sun sensitivity, infertility, stunted growth, and upper respiratory infection, and gastrointestinal infections commonly associated with decreased immunoglobulin levels. The syndrome is associated with immunodeficiency of a generalized type, ranging from mild and essentially asymptomatic to severe. Chromosomal abnormalities are hallmarks of the disorder, and high frequencies of sister chromatid exchanges and quadriradial configurations in lymphocytes and fibroblasts are diagnostic features. BS is caused by mutations in BLM , a member of the RecQ helicase family.

We determined whether BLM deficiency has any effects on the cell growth and cell death in BLM-deficient cells and mice. BLM-deficient EB-virus-transformed cell lines from BS patients and embryonic fibroblasts from BLM-/- mice showed slower growth than with wild-type cells. BLM deficient cells showed abnormal p53 protein expression after irradiation. In BLM-/- mice, small body size, reduced number of fetal liver cells, and increased cell death were observed. BLM deficiency causes up-regulation of p53, double-strand break and apoptosis which are likely observed in

irradiated control cells. Slow cell growth and increased cell death may be one of the causes for the small body size associated with BS patients.

Introduction

Bloom syndrome (BS) is a rare genetic disorder caused by mutations in BLM, a member of the RecQ helicase family (1). There are five human RecQ-like proteins (RECQL1, BLM, WRN, RECQL4 and RECQ5), each having 3' to 5' DNA helicase activity but little sequence similarity outside the helicase motifs (2,3). Three of these helicases (BLM, WRN and Rothmund-Thomson) show genomic instability and cancer susceptibility, but each also has distinctive features (4,5). The unique features of BS are severe pre- and post natal growth retardation and a wide spectrum of cancers that develop at a young age. Other BS phenotypes include facial sun sensitivity, immunodeficiency, and male sterility/female subfertility (6,7). Compared with Werner syndrome, small body size is one of the characteristic features associated with BS patients.

Here, we determined whether BLM deficiency has any effects on the cell growth and cell death in BLM deficient cells and mice.

Materials and Methods

BS patient

AsOk, who was identified in BS registry number 97, was born at 2250 g. Cafe-au-lait spot and mandibular hypoplasia were prominent. A 3bp deletion was detected in the BLM sequence of AsOk DNA (8). This deletion caused the generation of a stop codon at amino acid 186.

Cell culture

EB-virus-transformed cell lines from BS patients and control subjects were previously reported. PBMCs were isolated from the heparinized blood of patients by gradient centrifugation in Ficoll-Paque (Pharmacia AB, Uppsala, Sweden). PBMCs were suspended at a density of 10^6/ml in culture medium consisting of RPMI 1640 supplemented with 10% heat-inactivated fetal calf serum, l-glutamine (2 mmol/L), penicillin (100 U/ml) and streptomycin (100 μ g/ml). PBMCs (10^6/ml) were cultured in the presence of 10 μ g/ml phytohemagglutinin (PHA) for 3 days (9).

Detection of p53 protein

PBMCs cultured with PHA for 3 days were irradiated (6 Gy). After 1 hour, the cells were collected by centrifugation and protein was extracted from the PBMCs. Using anti-human p53 antibody (Santacruz, USA), immunoblotting was performed.

BLM-deficient embryonic fibroblasts

Heterozygous BLM deficient (BLM+/-) mice were kindly provided by P. Leder. BLM-/- mice were obtained by mating of BLM +/- mice (10). Embryonic fibroblasts from BLM-/- mice were obtained from 12.5-day embryos. None of the BLM-/- embryos could survive over 13 days.

Cell proliferation assay

Cell proliferation and cell viability were determined by trypan blue or MTT assay. MTT assay was performed following the manufacture's protocol. Embryonic fibroblasts were cultured with methyl methanesulfonate (MMS) (Sigma, Japan) for 24 hours (11). Then, the viable cell number was determined with trypan blue.

Detection of single strand DNA

Paraffin and cryostat sections were prepared from the brain of BLM +/- or -/- mice at 12.5 days postcoitus. Polyclonal rabbit anti-ssDNA antibody (IgG, 100 μg/ml, Dako Japan, Kyoto, Japan) 1:300 dilution was used to detect the formation of single-stranded DNA (ssDNA) at dilution 1:300 for 1 hr at room temperature. Immunoreactivity was detected with peroxidase-labeled- goat anti-rabbit immunoglobulins.

Results

Abnormal regulation of p53 protein expression

After the irradiation of PHA-stimulated PBMCs, p53 protein expression was induced in control cells (Fig. 1). In the BS patient's PBMCs, high p53 protein expression was detected even without irradiation. Irradiation slightly induced p53 protein in BS cells. In the BS EB cell line, p53 phosphorylation by ATM was up-regulated compared with that in the control EB cell line (data not shown). These results suggested that BLM-deficient cells have abnormal regulation of p53 protein expression and elevated frequency of apoptosis. Next, we investigated the apoptosis in vivo and in vitro using BLM deficient cells.

Slow growth in BLM-deficient cells

The growth rate of EB cells from BS patients was slower than that of control cells (Fig. 2). After irradiation, the growth rate of BS cells was slower than that of control cell. MMS action causes double-stranded DNA breaks. The sensitivity of BLM -/- cells to MMS was higher than that of wild type cells. Embryonic fibroblasts originating from BLM-/- mice also showed slow growth rate.

Augmented cell death in embryonic brain of BLM-/- mice

Anti-single-stranded DNA was detected in the brain of BLM-/- mice with the number being higher than that detected in the brain of BLM+/- mice (Fig. 3). This result suggested the augmented cell death in BLM -/- mice.

Discussion

In this study, we showed the abnormal regulation of p53 protein expression and augmented cell death in BLM-deficient cells both in vitro and in vivo. Stalled replication forks can result in double-strand breaks thereby triggering the activation of ATM (12). Consistent with a previously reported study, the deficiency of BLM is radiomimetic (13).

Originally, MMS was considered to directly cause double-stranded DNA breaks, because homologous-recombination-deficient cells are particularly vulnerable to the effects of MMS. However, it is now considered that MMS stalls replication forks, and cells that are homologous-recombination-deficient have difficulty repairing the damaged replication forks.

Studies in yeast and human cells suggest a pivotal role of RECQ-like helicases in maintaining genomic integrity during the S phase (14). BS patients show small body size from birth. This small size body continues over their life time. At 12.5 days postcoitus, BLM-deficient mice have smaller body size than wild-type mice (10).

BLM deficiency renders cells highly susceptible to apoptosis, suggesting a possible explanation for the pre- and postnatal growth retardation observed in BS patients. In the absence of BLM, many cells fail to repair the damage rapidly enough, whereupon p53 signals those cells to die. Individuals with BS may continually lose cells, owing to excessive apoptosis, particularly during pre- and postnatal development, when cell proliferation is excessive (15). Excessive apoptosis would leave many tissues with chronic cellular insufficiency, and hence, a small size, thereby explaining the pre- and postnatal growth retardation.

p53 is crucial for the apoptosis of BS cells. This apoptosis is not accompanied by an increase in BAX or p21 protein expression. Thus, p53 may induce apoptosis independent of its transactivation activity, consistent with the finding that p53 is transcriptionally inactive during the S phase. p53 may mediate the death of damaged BS cells by directly inducing mitochondria-mediated apoptosis or because of its transactivation activity.

In conclusion, BLM deficiency causes dysregulation of p53 and augmented apoptosis similarly to that in irradiated wild-type cells. These slow cell growth and increased cell death may cause the small body size associated with BS patients.

Figure legends

Fig. 1 p53 protein expression in PBMCs from a control subject and a BS patient.
PBMCs cultured with PHA for 3 days were irradiated (6 Gy). After 1 hour, cells were collected and p53 protein expression was detected.

Fig. 2 Cell proliferation and cell viability were determined using trypan blue. Embryonic fibroblasts were established from BLM +/- and BLM-/- mice at 12.5 days postcoitus. Embryonic fibroblasts from BLM-/- showed a slow growth rate and a high sensitivity to MMS compared with those from BLM+/- mice.

Fig. 3 Detection of single-stranded DNA. Immunohistochemical staining of BLM +/- and BLM-/- embryo at 12.5 days post coitus was performed.

References

1) Ellis, N.A., Groden, J., Ye, TZ., Straughen, J., Lennon, D.J., Ciocci, S., Proytcheva, M. and German, J. The Bloom's syndrome gene product is homologous to RecQ helicases. Cell 83: 655-666 (1995).

2) Ellis NA, Sander M, Harris CC, Bohr VA.
Bloom's syndrome workshop focuses on the functional specificities of RecQ helicases. Mech Ageing Dev. 129:681-91(2008)

3) Rossi ML, Ghosh AK, Bohr VA.
Roles of Werner syndrome protein in protection of genome integrity. DNA Repair (Amst). 9:331-44 (2010)

4) German J: Bloom syndrome: a Mendelian prototype of somatic mutational disease.

Medicine 72: 393-406 (1993)
5) Kaneko H, Kondo N. Clinical features of Bloom syndrome and function of the causative gene, BLM helicase Expert Rev Mol Diagn 4: 393-401 (2004)
6) German J: Bloom's syndrome. Dematol Cli 13: 7-18 (1995)
7) German J, Ellis NA: Bloom syndrome. In: The Genetic Basis of Human Cancer. Vogelstein B and Kinzler (eds.) McGraw-Hill, New-York, pp301-315 (1998)
8) Kaneko H, Isogai K, Fukao T, Matsui E, Kasahara K, Yachie A, Seki H, Koizumi S, Arai M, Utunomiya J, Miki Y, Kondo N. :Relatively common mutations of the Bloom syndrome gene in the Japanese population. Int J Mol Med 14:439-42. (2004)
9) Kaneko H, Matsui E, Fukao T, Kasahara K. Morimoto W, Kondo N. :Expression of BLM gene in human hematopoietic cells. Clin Exp Immunol 118: 285-289 (1999)
10) mice
11) Lundin C, North M, Erixon K, Walters K, Jenssen D, Goldman ASH, Helleday T. Methyl methanesulfonate (MMS) produces heat-labile DNA damage but no detectabe in vivo DNA double-strand breaks. Nucleic Acids Research 33; 3799-3811 (2005)
12) Beamish H, Kedar P, Kaneko H, Chen P, Fukao T, Peng C, Beresten S, Gueven N, Purdie D, Lees-Miller S, Ellis N, Kondo N, Lavin MF.
Functional link between BLM defective in Bloom's syndrome and the ataxia-telangiectasia mutated protein, ATM. J Biol Chem 277:30515-30523 (2002)
13) radionincent
14) Oh SD, Lao JP, Hwang PY, Taylor AF, Smith GR, Hunter N BLM ortholog, Sgs1, prevents aberrant crossing-over by suppressing formation of multichromatid joint molecules. Cell. 130:259-72 (2007)
15) Dvalos AR. And Campis J. Bloom syndrome cells undergo p53-dependent apoptosis and delayed assembly of BRCA1 and NSB1 repair complexes at stalled replication forks. J Cell Biol 29, 1197-1209 (2003)

Fig.1

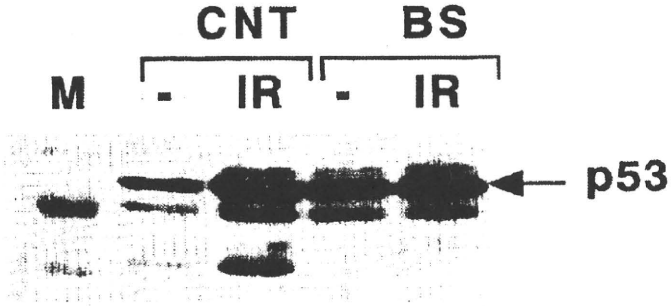

Fig. 3

BLM+/-

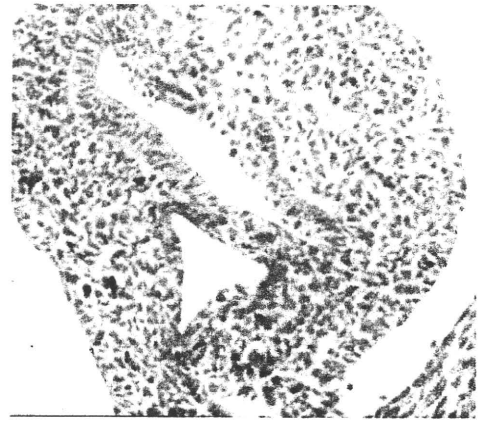

BLM-/-

Fig. 2

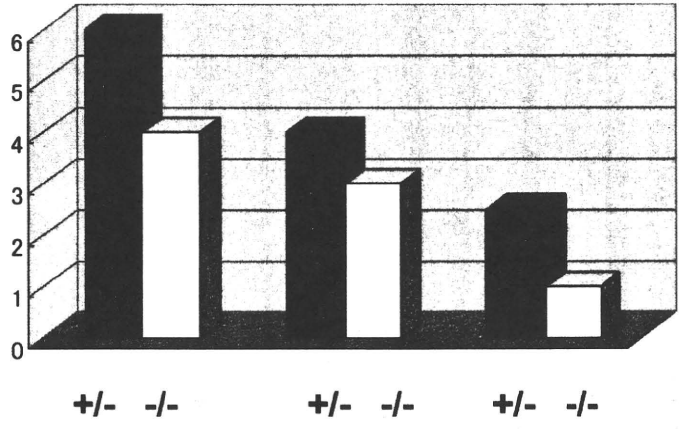

Thrombosis Research 125 (2010) e17–e22

Contents lists available at ScienceDirect

Thrombosis Research

journal homepage: www.elsevier.com/locate/thromres

Regular Article

A family having type 2B von Willebrand disease with an R1306W mutation: Severe thrombocytopenia leads to the normalization of high molecular weight multimers

Michio Ozeki [a,*], Shinji Kunishima [b], Kimiko Kasahara [a], Michinori Funato [a], Takahide Teramoto [a], Hideo Kaneko [a], Toshiyuki Fukao [a], Naomi Kondo [a]

[a] Department of Pediatrics, Gifu University Graduate School of Medicine, Gifu, Japan
[b] Department of Advanced Diagnosis, Clinical Research Center, National Hospital Organization Nagoya Medical Center, Nagoya, Japan

ARTICLE INFO

Article history:
Received 8 March 2009
Received in revised form 9 August 2009
Accepted 10 August 2009
Available online 8 September 2009

Keywords:
type 2B von Willebrand disease
von Willebrand factor
giant platelets
thrombocytopenia
polymorphism

ABSTRACT

In type 2B von Willebrand disease (2B VWD), abnormal von Willebrand factor (VWF) spontaneously binds to platelets. This leads to the clearance of the high molecular weight multimers (HMWM) of VWF and results in thrombocytopenia. Herein we report a family of 2B VWD with an R1306W mutation which caused thrombocytopenia with giant platelets. The most important finding in this study is dynamic changes in VWF values in association with platelet counts. When the proband (2 years of age) had severe thrombocytopenia, his HMWM were normal, however, hematological examination showed a low level of VWF and a lack of HMWM after platelet count recovered. His affected sister also exhibited similar phenomenona. These results suggest that the severe thrombocytopenia leads to decreased clearance of VWF HMWM and restoration of VWF HMWM in plasma. We must consider 2B VWD in the case of recurrent thrombocytopenia following infection or other stress condition.

Introduction

Von Willebrand disease (VWD) is a common heterogeneous bleeding disorder and is represented by a reduction and/or abnormal function of the von Willebrand factor (VWF) [1]. In type 1 and 3 VWD, deficiencies or the absence of the vWF protein are responsible for the bleeding syndrome. Type 2 VWD is characterized by a wide heterogeneity of functional and structural deficits. Type 2B VWD (2B VWD) is caused by the increasing binding affinity of VWF for platelet glycoprotein Ib (GPIb) and is characterized by the relative loss of VWF high molecular weight multimers (HMWM) in plasma [2]. Though patients with 2B VWD often have diverse symptoms, including moderate to severe thrombocytopenia, giant platelets and spontaneous platelet agglutination, the degree of these reported symptoms is highly variable [3]. Thrombocytopenia associated with 2B VWD is not a rare finding, especially in children [4]. It is found to be transient or persistent with variable platelet counts on different occasions. It is known that infusion of desmopressin (DDAVP) can induce the release of VWF from endothelial cells [5]. Other situations, such as physiological (pregnancy) or pathological (infections, surgeries) stress conditions, also induce the release of VWF in 2B VWD plasma [6,7]. These events are associated with the occurrence of thrombocytopenia and spontaneous platelet agglutination in 2B VWD. Saba et al. referred to 2B VWD patients with giant platelets, chronic thrombocytopenia and spontaneous platelet agglutination as type 2B Tampa [8].

The VWF gene, located on the short arm of chromosome 12 spans 178 kb in length and contains 52 exons. There is a pseudogene on chromosome 22 corresponding to VWF exons 23–34. These sequences have about 97% homology, which makes it difficult to detect mutations in these regions [9]. The gain of functional mutations in exon 28 of the VWF gene encoding the VWF A1 domain is reported to be responsible for 2B VWD.

Herein we present a family of type 2B VWD with an R1306W mutation which caused severe thrombocytopenia with giant platelets. We describe the mutation analysis of this family and the dynamic changes in their platelet count, VWF and HMWM, which are useful for understanding the mechanism of the loss of VWF HMWM and severe thrombocytopenia in 2B VWD.

Patients

The proband

The proband was a 2-year-old Japanese boy who was admitted to our hospital due to presenting several purpura spots on the elbow following acute bronchitis. The patient's father had a past medical history of idiopathic thrombocytopenic purpura (ITP) during childhood. A hematological examination revealed thrombocytopenia (16,000/μl) measured by automated counter. PT was 83% (normal range: 70–120%), APTT was 45.0 s (normal range: 25.0–43.0 s) and

* Corresponding author. Department of Pediatrics, Gifu University Graduate School of Medicine. Yanagido 1-1, Gifu 501-1194, Japan. Tel.: +81 58 2306386; fax: +81 58 2306387.
E-mail address: mi_ti_ti_1227@yahoo.co.jp (M. Ozeki).

0049-3848/$ – see front matter © 2009 Elsevier Ltd. All rights reserved.
doi:10.1016/j.thromres.2009.08.012

fibrinogen was 320 mg/dl (normal range: 150–350 mg/dl). Ristocetin cofactor activity was within the normal limit (151%). Platelet-associated IgG (PAIgG) was 85.7 ng/10^7 platelets (normal range: 9.0–25.0 ng/10^7 platelets). A blood smear showed that most platelets were enlarged, most of them close to the size of red blood cells, some even larger than erythrocytes (Fig. 1A). Review of the bone marrow aspirate confirmed the normal number and morphology of megakaryocytes. The patient was tentatively diagnosed as ITP. A high-dose immunoglobulin therapy (1 g/kg) was done, but the platelet count remained at a low-level for a week. Because of the familial history and giant platelets in peripheral blood, the patient was considered as having inherited thrombocytopenia with giant platelets (macrothrombocytopenia). Immunomorphological evaluation of myosin IIA distribution within granulocyte cytoplasm excluded *MYH9* disorders [10]. Flow cytometry for platelet GPIb expression excluded Bernard-Soulier syndrome [11]. The platelet count was gradually increased to more than 100,000/μl and the patient was discharged. The diagnosis was uncertain at that time. Within half a year, the patient experienced several episodes of prolonged and excessive nasal hemorrhage and thrombocytopenia, 1 to 3 weeks after acute viral infection. The platelet count was recovered spontaneously without therapy. When the platelet count was 264,000/μl during the third hospitalization, hematological examinations showed factor VIII coagulant activity (VIII:C), von Willebrand factor antigen (VWF:Ag) and von Willebrand factor ristocetin cofactor (VWF:RCo) decreased; 50%, 40%, 13%, respectively. The electrophoretic pattern obtained from the patient's plasma showed a lack of VWF HMWM. In the following year, we observed a similar finding in the proband when he suffered from high fever and nasal hemorrhage associated with influenza A virus infection. A hematological examination revealed thrombocytopenia (52,000/μl) and VWF multimer pattern was normal. As his platelet count increased (179,000/μl) after a week, he lost the VWF HMWM and his VWF: Ag decreased.

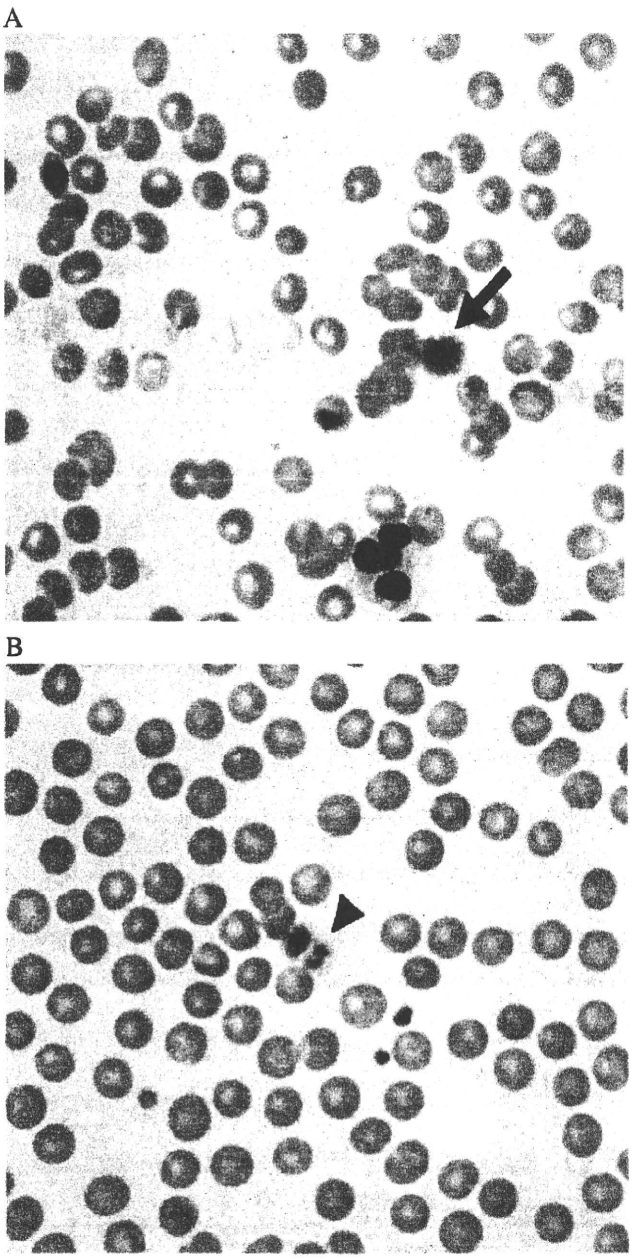

Fig. 1. Platelet morphology on peripheral blood smears (light microscopical images of peripheral blood films after May-Giemsa stain). A. The platelets of the patient are larger than red blood cells (arrow). B. The platelets of his father are also enlarged, but smaller than those of the patient (arrowhead).

His father

His father had a history of bleeding characterized by mucosal bleeding and purpura in childhood and was diagnosed with ITP. His platelet count was 100,000/μl, he had a low-level of VIII:C, VWF:Ag and VWF:RCo and enlarged platelets on a peripheral blood smear (Fig. 1B). The plasma VWF showed a loss of VWF HMWM.

His elder sister

The patient's 5-year-old sister experienced severe bronchitis induced by respiratory syncytial (RS) virus infection. Though she had no symptoms of a hemorrhagic state, severe thrombocytopenia (9,000/μl) and giant platelets on a peripheral blood smear were noted (data not shown). Her factor VIII-related activities were within normal limits. The thrombocytopenia improved for a few days without therapy. When the platelet count was 197,000 /μl, her VWF:RCo was low-level. Her plasma VWF showed a loss of VWF HMWM.

Materials and Methods

PCR amplification and sequencing of VWF gene

Informed consent for the study was obtained from his parents. Genomic DNA was isolated from EDTA anticoagulated peripheral blood mononuclear cells, obtained from the patient and his family members according to standard procedures [12]. The exon 28 of the VWF gene was amplified using previously reported primers [9].

Primer U1 intron 27 g7525–7544: sense 5′-TGGGAATATGGAAGT CATTG-3′,

Primer U2 intron 27 g7504–7523: sense 5′- GGTGGAACAGAGGAG ATTCT-3′,

Primer L1 exon 28 g8150–8169: antisense 5′- TGACCTTCTTCTTCTT CAGG-3′,

Primer L2 exon 28 g8129–8147: antisense 5′- CTGGACGTAGCGGA CAAAG-3′.

Four base-mismatches with the VWF pseudogene in the U1 primer are underlined. The primers of U2 and L2 were designed to amplify the fragments of both the VWF gene and the pseudogene. The PCR conditions were initial denaturation at 95 °C followed by 40 cycles of 30 seconds of denaturation at 95 °C, 30 seconds of annealing at 58 °C, 45 seconds of polymerization at 72 °C, and finally 10 min of extension at 72 °C. A PCR fragment was directly sequenced with an ABI PRISM

3100 Genetic Analyzer (Applied Biosystems, Foster City, CA). In the case of fragments amplified by U2 and L2 primers, sequencing was done after subcloning into plasmid vectors using a Mighty cloning kit (Takara Bio, Ohtsu, Japan).

RT-PCR

RNA was isolated from the platelet pellet by using an RNA isolation kit (Isogen, Nippon Gene, Tokyo, Japan) and cDNA was synthesized with oligo dT primers and SuperScript II Reverse Transcriptase (Invitrogen, Carlsbad, CA). The PCR products were amplified using U3 (exon 27 g5430–5448: sense 5′-TCCCAGTGACCCTGAGCAC-3′) and L2.

Result

Functional diagnosis of 2B VWD

The proband showed a lack of VWF HMWM. We performed a ristocetin-induced platelet agglutination (RIPA) study. The addition of ristocetin at a low concentration (0.5 mg/ml) resulted in platelet agglutination to the proband's platelet-rich plasma (PRP) but not in normal PRP, and 1.25 mg/ml of ristocetin induced an almost full agglutination in even the control PRP (Fig. 2A and B). This suggests that PRP from the patient was more sensitive to the induction of platelet agglutination by the low concentration of ristocetin. These findings are typical of previous findings in type 2B and platelet-type VWD [1]. To distinguish these conditions, a mixing study was performed. The proband's platelets did not show enhanced RIPA when they were suspended in control plasma (Fig. 2C); in contrast, the proband's plasma with control platelets caused enhanced RIPA at 0.5 mg/ml of ristocetin (Fig. 2D). Therefore, the patient was diagnosed with 2B VWD. In addition, a study of the sister's sample showed the same results (data not shown).

Mutation analysis of the family

The DNA fragments of exon 28 in the VWF gene from the proband and his family were amplified by using the primer pair U1 and L1, which were reported to be specific for the active gene sequence. A heterozygous mutation c.4166C>T (g.7859C>T, R1306W) was identified in the proband by direct sequencing, as shown in Fig. 3. However, this mutation was not detected in the affected sister and the father by direct sequencing. To study the discrepancy between gene analysis and their phenotypes, PCR was performed using other primer pairs, U2 and L2, which could amplify exon 28 fragments from both the VWF gene and the pseudogene. After subcloning PCR products from the proband, 16 independent clones were sequenced. Five of them were revealed to be derived from the pseudogene by comparison of sequence differences between the functional VWF gene and its pseudogene. Out of 11 clones derived from the functional VWF gene, 4 clones had c.4166C>T (g.7859C>T, R1306W) and 7 clones did not. In addition, all clones derived from the functional gene had a g.7541A>G substitution (a prevalent polymorphism) within primer U1 (intron 27) which identified both alleles. Familial analysis using this method revealed that this polymorphism was identified in the fragment with c.4166C>T (g.7859C>T, R1306W) but not in the fragment without c.4166C>T in both the father and sister. We concluded that this polymorphism on the site of the U1 primer hindered amplification of the mutant allele with this polymorphism (father and sister) although mutant and normal alleles were amplified with similar efficiency in the case of a homozygote of this polymorphism (the proband) (Fig. 4). We further confirmed the

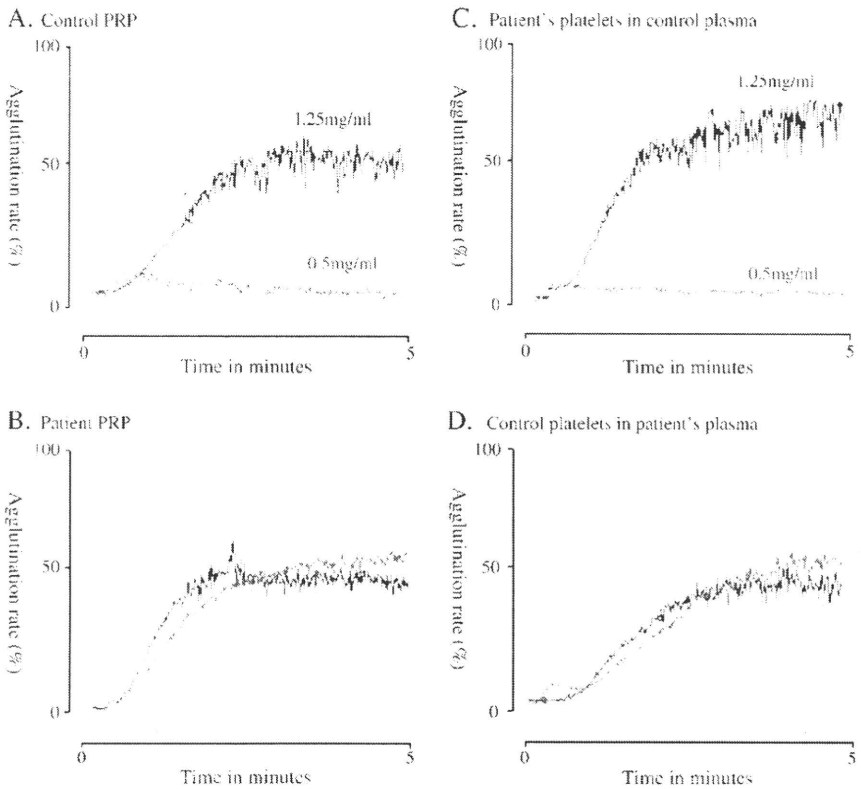

Fig. 2. Ristocetin-induced-platelet agglutination (RIPA) and mixing analysis. A. control PRP; B. patient PRP; C. patient platelets in control plasma; D. control platelets in patient plasma; Values within figure represent ristocetin concentrations (mg/ml).

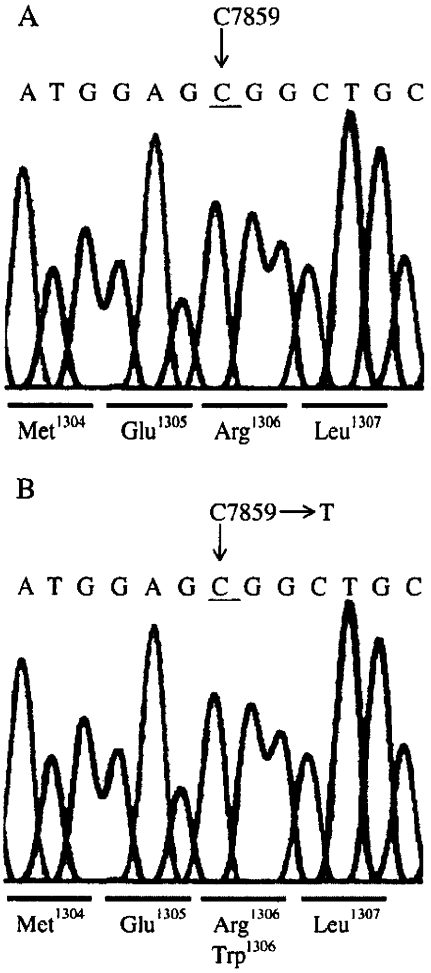

Fig. 3. DNA sequence analysis of an amplified fragment of exon 28 of the VWF gene. A. control, B. the proband.

heterozygous c.4166C>T (g.7859C>T, R1306W) mutation in the proband, the sister and the father by RT-PCR using primer U3 and L2.

Dynamic changes in platelet count and values in VWF analyses

Fig. 5 shows the laboratory data and the multimer electrophoresis analysis of the plasma VWF in the family. The multimer pattern of the proband with at the time of severe thrombocytopenia demonstrated an almost normal pattern, together with normal values of VIII: C, VWF: Ag and VWF: Rco. The multimer pattern with an adequate platelet count clearly showed a lack of HMWM. At the same time, the values of VIII: C, VWF: Ag and VWF: Rco were low. This pattern was observed twice independently in the proband. The multimer pattern and VWF study of the sister demonstrated a similar pattern. When the sister was affected by severe bronchitis with an RS virus infection, her VIII: C, VWF: Ag and VWF: Rco were within normal limits and HMWM were present. However, when the platelet count was normalized after bronchitis, her values of VIII: C, VWF: Ag and vWF: Rco had decreased and the multimer pattern lacked HMWM. The study of the father without symptoms showed a low level of VIII: C, VWF: Ag and VWF: Rco and a lack of HMWM.

Discussion

Here we presented a family with 2B VWD characterized by the presence of a heterozygous R1306W substitution in the VWF A1 domain.

First, we should caution about exon 28 amplification of active VWF gene. The DNA fragments of exon 28 in the VWF gene have been widely amplified by the pair of primers U1 and L1 [13]. These primers can amplify the active VWF gene but not the pseudogene because U1 includes four different nucleotides from the pseudogene sequences at its 3′ ends. However, there is a prevalent A to G polymorphism at g.7541. In an Asian population, the frequency of A at nucleotide 7541 is 0.411, and that of G is 0.589 (Reference SNP: rs216312). This polymorphism is located in the fourth nucleotide from the 3′ end of primer U1, hinders PCR amplification in case of the G allele and results in misunderstanding of mutation status (Fig. 4). Two previous reports

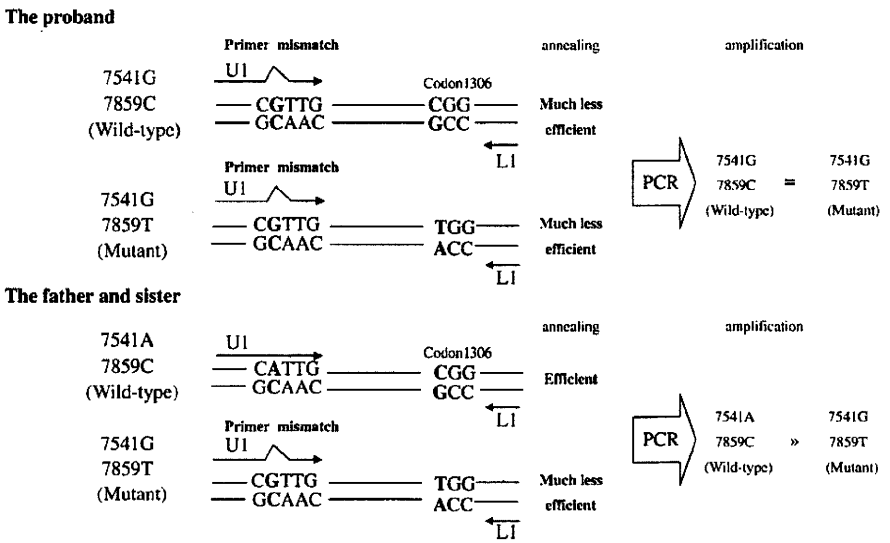

Fig. 4. Schematic illustration of problematic amplification of exon 28 using U1 and L1 primers in the presence of a g.7851A>G polymorphism.There is a prevalent polymorphism at g.7541A>G. Primer U1 is designed to fit g.7541A. Primer U1 is much less effectively annealed to the fragment of the g.7541G allele than g.7541A because of nucleotide mismatch. The proband had 7541G in both alleles. Primer U1 was less effectively annealed to fragments from both alleles and fragments from both alleles were amplified with equal efficiency. Hence the 7859C>T mutation was easily detected by direct sequencing. The father and the sister had the 7541A allele with no mutation at 7859 and the 7541G allele with a 7859C>T mutation. In this case, the 7541A allele was much more effectively amplified than 7541G. Hence fragments of 7541A with no mutation at 7859 were predominant. Hence direct sequence mis-diagnosed the father and the sister as having no mutation at 7859.

	Control	Proband			Sister		Father
		(1)	(2)	(3) (4)	(1)	(2)	
Platelet count ($\times 10^4/\mu l$)	2.0	26.4	5.2	17.9	0.9	19.7	19.0
VIII:C (%) (NR: 60-150%)	108	50	56	31	181	45	37
VWF:Rco (%) (NR: 60-170%)	151	13	46	21	232	19	18
VWF:Ag (%) (NR: 50-155)	72	40	70	37	142	78	42

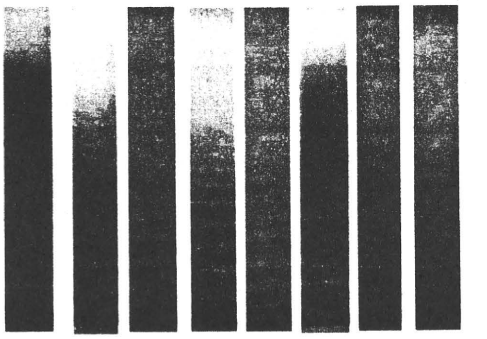

Fig. 5. Laboratory data and multimer electrophoresis pattern of plasma. Plasma VWF multimers analyzed by sodium dodecyl sulfate-agarose gel electrophoresis displayed selective reduction in the high molecular weight forms. Proband (1): On first admission, he had severe thrombocytopenia. (2): On third admission, his platelet count recovered. (3)(4): He suffered from high fever associated with influenza A virus infection and recovered after a week. Sister (1): She was affected by severe bronchitis-induced RS virus infection. (2): Her platelet count was normalized after bronchitis recovery. Father: a screening examination without symptoms. NR - normal range. VIII:C - factor VIII coagulant activity. VWF:Ag - von Willebrand factor antigen. VWF:Rco - von Willebrand factor ristocetin cofactor.

also pointed out this phenomenon [13,14]. RT-PCR or additional genomic PCR as described in this paper is necessary for mutation analysis.

The mutations in the VWF A1 domain that cause 2B VWD can influence phenotype [15]. Previous studies with recombinant proteins mutated at different residues have confirmed that they bind with different affinities to GPIb [16]. The R1306W mutation that we found in our family was first reported in 1991 [17]. Cooney et al. demonstrated that the R1306W mutation is sufficient to confer increased binding of large VWF multimers to platelet GPIb, resulting in the 2B VWD phenotype, and sufficient to produce the specific type 2B "gain-of-function" phenotype, and confirms that no other factors relating to VWF posttranslational processing or secretion in endothelial cells are required for this effect [18]. Another study demonstrated that the R1306W mutation produced similar binding of the VWF to platelets both spontaneously and when induced by ristocetin [19].

Federici et al. reported a cohort study of 67 2B VWD patients from 38 unrelated families for 48 months [15]. Thrombocytopenia was found in 20 patients (30%) at baseline and in 38 (57%) after stress conditions were observed. According to the report, phenotypic variation was associated with genotypes. Patients with H1268H, R1306W, R1308C, I1309V, V1316M or R1341Q/W had thrombocytopenia after stress but patients with P1266L or R1308L did not. In the study, 15 patients (9 families) with the R1306W mutation, aged 14–77 years (median 43 years), were followed-up. Their platelet counts at base line was 165 (54–214) $\times 10^3/\mu l$ and the platelet morphology was enlarged platelets without aggregates, as with our patients. During pregnancy, infections and surgery, patients with the R1306W mutation had thrombocytopenia with median trough platelet counts of 56 (n = 4), 85 (n = 2), and 73 (n = 3) $\times 10^3/\mu l$, respectively. Our proband (2 years old) and his sister (5 years old) who also had the R1306W mutation developed more severe thrombocytopenia than the patients in that report. The physiologic factors, age, sex, blood group, pregnancy, and exercise are factors that influence plasma VWF levels and that may thus affect a type 2B VWD phenotype and differentially influence its diagnosis [20]. Maybe age is a factor influencing the severity of thrombocytopenia in this genotype.

One of the important findings in this study is dynamic changes in VWF values in association with platelet count. When the patient had severe thrombocytopenia, his HMWM were normal, however, hematological examination showed a low level of VWF and a lack of HMWM after platelet count recovered. His sister exhibited similar phenomenona. Although a cohort study of a large number of type 2B cases including 15 patients with the same R1306W mutation did not found this dynamic changes in VWF values in association with platelet count, all the patients with R1306W mutation in the study were much older (14–77 y) than our sibling case. We could not find such dynamic change in their father with the same mutation. Hence we speculate that dynamic changes in VWF values in association with platelet count are also age-dependent. This phenomenon could be explained as follows: Since VWF is an acute phase reactant [6,7], a large number of mutant VWF are expected to be released from vascular endothelial cells in acute phase of infection. This induction may facilitate platelet agglutination and increased clearance of platelet- VWF complex and result in thrombocytopenia. If VWF induction lasts in the condition of thrombocytopenia, this may lead to decreased clearance of VWF and restoration of mutant VWF HMWM. Similar phenomenona were reported very recently in a patient with 2B VWD complicated by ITP with a different mutation from ours [21].

The present case presented macrothrombocytopenia at admission. Inherited forms of giant platelet disorders or congenital macrothrombocytopenia are rare. Recent research demonstrated that clinical laboratory-based tests might differentiate at least half of undifferentiated macrothrombocytopenia [11]. The most common congenital macrothrombocytopenia includes *MYH9* disorders and the Bernard-Soulier syndrome, however, 2B VWD must be considered because about 30% of the patients with 2B VWD have giant platelets.

From the lesson of our study, it is important to consider 2B VWD in the case of recurrent thrombocytopenia following acute viral infection or other stress, with giant platelets and/or a familial history of thrombocytopenia. Our present study clearly indicates the importance of studying VWF during a patient's non thrombocytopenic condition.

Conflict of interest statement

The authors have no conflict of interest.

Acknowledgements

This work was supported by grants to S.K. from the Japan Society for the Promotion of Science, the Ministry of Health, Labor and Welfare (Grant for Child Health and Development 19C-2), Charitable Trust Laboratory Medicine Foundation of Japan, Mitsubishi Pharma Research Foundation, and National Hospital Organization Research Fund.

We thank Ms. Yoshimi Ito for her skillful technical assistance.

References

[1] Schneppenheim R, Thomas KB, Sutor AH. Von Willebrand disease in childhood. Semin Thromb Hemost 1995;21(3):261–75.
[2] Werner EJ. Von Willebrand disease in children and adolescents. Pediatr Clin North Am 1996;43(3):683–707.
[3] Nurden P, Debili N, Vainchenker W, Bobe R, Bredoux R, Corvazier E, et al. Impaired megakaryocytopoiesis in type 2B von Willebrand disease with severe thrombocytopenia. Blood 2006;108:2587–95.

[4] Noris P, Pecci A, Bari FD, Stazio MT, Pumpo MD, Ceresa IF, et al. Application of a diagnostic algorithm for inherited thrombocytopenias to 46 consecutive patients. Haematologica 2004;89:1219–25.
[5] Holmberg L, Nilsson IM, Borge L, Gunnarsson M, Sjorin E. Platelet aggregation induced by 1-desamino-8-arginine vasopressin (DDAVP) in Type 2B von Willebrand's disease. N Engl J Med 1983;309:816–21.
[6] Rick ME, Williams SB, Sacher RA, McKeown LP. Thrombocytopenia associated with pregnancy in a patient with type 2B von Willebrand's disease. Blood 1987;69:786–9.
[7] Hultin MB, Sussman II. Postoperative thrombocytopenia in type IIB von Willebrand disease. Am J Hematol 1990;75:86–91.
[8] Saba HI, Saba SR, Dent J, Ruggeri ZM, Zimmerman TS. Type 2B Tampa: A variant of von Willebrand disease with chronic thrombocytopenia, circulating platelet aggregates and spontaneous platelet aggregation. Blood 1985;66:282–6.
[9] Mancuso DJ, Tuley EA, Westfield LA, Lester-Mancuso TI, Le Beau MM, Sorace JM, et al. Human von Willebrand factor gene and pseudogene: Structual analysis and differentiation by polymerase chain reaction. Biochemistory 1991;30:253–69.
[10] Kunishima S, Matsushita T, Kojima T, Sako M, Kimura F, Jo EK, et al. Immunofluorescence analysis of neutrophil nonmuscle myosin heavy chain-A (NMMHCA) in *MYH9* disorders: association of subcellular localization with *MYH9* mutations. Lab Invest 2003;83:115–22.
[11] Kunishima S, Saito H. Congenital macrothrombocytopenias. Blood Rev 2006;20:111–21.
[12] Blin N, Stafford DW. A general method for isolation of high molecular weight DNA from eukaryocytes. Nucleic Acid Res 1976;3:2303–8.
[13] Kanaji T, Okamura T, Kuroiwa M, Murakawa M, Kamura T, Niho Y. A sequence analysis of von Willebrand factor mRNA, gene, and pseudogene in two patients with von Willebrand disease type 2B, and an investigation of gene conversion in its gene. Int J Hematol 1996;64:53–9.
[14] Eikenboom JCJ, Reitsma PH, Briet E. Seeming homozygosity in type-2B von Willebrand's disease due to a polymorphism within the sequence of a commonly used primer. Ann Hematol 1994;68:139–41.
[15] Federici AB, Mannucci PM, Castaman G, Baronciani L, Bucciarelli P, Canciani MT, et al. Clinical and molecular predictors of thrombocytopenia and risk of bleeding in patients with von Willebrand disease type 2B: a cohort study of 67 patients. Blood 2009;113:526–34.
[16] De Romeuf C, Hilbert L, Mazurier C. Platelet activation and aggregation induced by recombinant von Willebrand factors reproducing four type 2B von Willebrand disease missense mutations. Thromb Haemost 1998;79:211–2.
[17] Cooney KA, Nichols WC, Bruck ME, Bahou WF, Shapiro AD, Bowie EJ, et al. The molecular defect in type 2B von Willebrand disease. Identification of four potential missense mutations within the putative GPIb binding domain. J Clin Invest 1991;87:1227–33.
[18] Cooney KA, Lyons SE, Ginsburg D. Functional analysis of a 2B von Willebrand disease missense mutation: Increased binding of large von Willebrand factor multimers to platelets. Proc Natl Acad Sci 1992;89:2869–72.
[19] Cooney KA, Ginsburg D. Comparative analysis of type 2b von Willebrand disease mutations: implications for the mechanism of von Willebrand factor binding to platelets. Blood 1996;87:2322–8.
[20] Othman M, Favaloro EJ. Genetics of type 2B von Willebrand disease: "true 2B," "tricky 2B," or "not 2B." What are the modifiers of the phenotype? Semin Thromb Hemost 2008;34:520–31.
[21] Wang ZJ, Onwuzurike N, Callaghan MU, Rajpurkar M, Chitlur M, Lusher JM. Decreased clearance of von Willebrand factor in a patient with type 2B von Willebrand disease following development of immune thrombocytopenia. Pediatr Blood Cancer 2008;51:416–8.

Expression of ADAMTS4 in Ewing's sarcoma

K. MINOBE[1,2], R. ONO[1*], A. MATSUMINE[3*], F. SHIBATA-MINOSHIMA[2], K. IZAWA[2], T. OKI[2], J. KITAURA[2], T. IINO[3], J. TAKITA[4], S. IWAMOTO[5], H. HORI[5], Y. KOMADA[5], A. UCHIDA[3], Y. HAYASHI[6], T. KITAMURA[2] and T. NOSAKA[1]

[1]Department of Microbiology and Molecular Genetics, Mie University Graduate School of Medicine, Tsu; [2]Division of Cellular Therapy, The Institute of Medical Science, The University of Tokyo, Tokyo; [3]Department of Orthopaedic Surgery, Mie University Graduate School of Medicine, Tsu; [4]Department of Cell Therapy and Transplantation Medicine, Graduate School of Medicine, The University of Tokyo, Tokyo; [5]Department of Pediatrics and Developmental Science, Mie University Graduate School of Medicine, Tsu; [6]Gunma Children's Medical Center, Gunma, Japan

DOI: 10.3892/ijo_xxxxxxxx

Abstract. Ewing's sarcoma (EWS) is a malignant bone tumor that frequently occurs in teenagers. Genetic mutations which cause EWS have been investigated, and the most frequent one proved to be a fusion gene between *EWS* gene of chromosome 22 and the *FLI1* gene of chromosome 11. However, a limited numbers of useful biological markers for diagnosis of EWS are available. In this study, we identified ADAMTS4 (a disintegrin and metalloproteinase with thrombospondin motifs) as a possible tumor marker for EWS using the retrovirus-mediated signal sequence trap method. ADAMTS4 is a secreted protein of 837 amino acids with a predicted molecular mass of 98-100 kDa. It is a member of metalloprotease family, is expressed mainly in cartilage and brain, and regulates the degradation of aggrecans. ADAMTS4 has been suggested to be involved in arthritic diseases and gliomas. Herein, we show that *ADAMTS4* mRNA was expressed in all primary EWS samples and all EWS-derived cell lines examined, while its expression was detected only in small subpopulations of other solid tumors. Furthermore, *ADAMTS4* expression was found to be regulated by *EWS-FLI1* fusion gene-dependent manner. We also demonstrated that ADAMTS4 protein was highly expressed in tumor samples of the patients with EWS by using immunohistochemistry. These results suggest that ADAMTS4 is a novel tumor marker for EWS.

Correspondence to: Dr T. Nosaka, Department of Microbiology and Molecular Genetics, Mie University Graduate School of Medicine, 2-174, Edobashi, Tsu 514-8507, Japan
E-mail: nosaka@doc.medic.mie-u.ac.jp

*Contributed equally

Key words: EWS-FLI1, tumor marker, signal sequence trap, retrovirus

Introduction

Ewing's sarcoma (EWS) is the second most frequent primary bone tumor of childhood and adolescence with aggressive clinical course and poor prognosis. It is recognized that EWS is a part of Ewing's sarcoma family of tumors (ESFTs) which also include the peripheral primitive neuroectodermal tumor (PNET) (1,2), Askin's tumor and extraosseous EWS. Biologically, ESFTs are characterized by common chromosomal translocation between the 5' portion of the *EWS* gene (22q12) and the 3' portion of the members of the *ETS* family genes (3). More than 85% of the cases have the fusion gene *EWS-FLI1* due to t(11;22)(q24;q12) (4,5). Five to 10% of the cases pocess *EWS-ERG* due to t(21;22)(q22;q12) (6). The other rare cases are *EWS-ETV1*, *EWS-E1AF* and *EWS-FEV*, each resulting from t(7;22)(p22;q12), t(17;22) (q12;q12) and t(2;22)(q33;q12), respectively (3,7,8). The EWS-ETS chimeric proteins behave as aberrant transcriptional regulators and are believed to play a crucial role in the onset and progression of the ESFTs (9,10).

Currently, diagnosis of EWS is determined mainly by CD99 immunohistochemistry (11-13), and by genetic aberration. However, CD99 expression is also reported to be positive in some T cell acute lymphoblastic leukemia (T-ALL), acute myelogenous leukemia (AML), ependymoma, synovial sarcoma and pancreatic endocrine tumors (14-16). Besides, not all EWSs have this specific chromosomal translocation. Thus, there is no specific biomarker for differentiating EWS from other soft tissue sarcomas. Among the patients with localized tumor at diagnosis, 20% relapse within 4 years and die of the disease. In contrast, 5-year survival rate is ~20-30% in cases with metastasis. This study was performed to find a useful tumor marker for EWS.

The signal sequence trap (SST) is a strategy to identify complementary DNAs (cDNAs) containing signal sequence that encode secreted and type I membrane proteins (17). To date, various important molecules have been detected including *SDF-1*, a member of the tumor necrosis factor receptor superfamily *TROY*, *Xenopus-Tsukushi*, *Vasorin* and leukocyte mono-Ig-like receptor (*LMIR*) by the SST method

(18-23). In this study, we identified a secreted molecule *ADAMTS4* (a disintegrin and metalloproteinase with thrombospondin motifs) from EWS cell lines by using the SST system based on retrovirus-mediated expression screening (SST-REX) (24,25).

ADAMTS is a family of proteinases which was first described in 1997 (26). Today, 19 different members of the *ADAMTS* family have been identified, but the functions, mechanisms of activation, and substrates of most members remain incompletely understood (27). Members of the *ADAMTS* family are closely related to the *ADAM* (a disintegrin and metalloproteinase) family, but unlike *ADAMs*, the *ADAMTSs* are secreted molecules, some of which bind to the extracellular matrix. *ADAMTS4* was originally purified from chondrocytes and synovial cells stimulated with interleukin-1 (28). The structure of ADAMTS4 consists of six domains, a prodomain, a metalloproteinase domain, a disintegrin domain, a thrombospondin type I motif, a cysteine-rich domain and a spacer domain. It has been demonstrated to cleave the aggrecan at Glu^{373}-Ala^{374}, and therefore is also named as *aggrecanase1* (29-32). The aggrecanase activity of ADAMTS4 is inhibited by TIMP-3 (tissue inhibitor of metalloproteinase-3) (33), which was originally identified as an inhibitor of matrix metalloproteinases. Yamanishi *et al* demonstrated that *ADAMTS4* was overexpressed in synovial cells and chondrocytes in the patients with osteoarthritis (OA) and rheumatoid arthritis (RA) (34). Thus, *ADAMTS4* is considered to play an important role in the aggrecan degradation of articular cartilage in OA and RA. Recent studies reported that ADAMTS4 cleaves not only aggrecan but also brevican, versican and α2-macroglobulin (35).

In this study, we have disclosed that *ADAMTS4* mRNA was expressed in all tissue samples of EWS patients and all EWS cell lines examined, and the mRNA level of *ADAMTS4* was regulated by *EWS-FLI1* in the cell line. We have also demonstrated the ADAMTS4 protein expression by immunostaining of the patients' samples and the cell lines. Thus, we propose that ADAMTS4 is a possible tumor marker of EWS.

Materials and methods

Cell lines. Osteosarcoma cell lines (MG63, HOS, KHOS/NP, SaOS2 and U2OS), neuroblastoma cell lines (KPNSI-FA, LAN-1 and NB69), a lung cancer cell line H460, a liver cancer cell line PLC/PRF/5, a cholangiocarcinoma cell line HuCCT1, a colon cancer cell line SW-48, T-ALL cell lines (Jurkat, PEER, CEM and HPB-ALL), B-ALL cell lines (NALM16, NALM24 and IM9), AML cell lines (MOLM13 and ML1), an acute myelomonocytic leukemia cell line U937, EWS cell lines (SJES-2, SJES-3, SJES-5, SJES-6, SJES-7 and SJES-8), rhabdomyosarcoma cell lines (RMS and SJRH-30), pancreatic cancer cell lines (AsPC-1, BxPC-3 and Capan-1), glioblastoma cell lines (U87MG, U251 and T98G), and gastric cancer cell lines (HGC-27, MKN45, GCIY and KATO-III) were cultured in RPMI-1640 medium (Sigma-Aldrich, St. Louis, MO, USA) containing 10% heat-inactivated fetal bovine serum (FBS) (Sigma-Aldrich). A murine pro-B cell line Ba/F3 was maintained in RPMI-1640 containing 10% FBS and 1 ng/ml murine interleukin-3 (IL-3) (R&D Systems, Minneapolis, MN, USA). A retrovirus packaging cell line Plat-E (36) and NIH3T3 were cultured in Dulbecco's modified Eagle's medium (DMEM) (Sigma-Aldrich) containing 10% FBS. Human mesenchymal stem/progenitor cells (hMSCs) were purchased from Sanko Junyaku (Tokyo, Japan).

Patient samples and normal controls. Samples from 7 patients with EWS, 13 osteosarcoma, 4 chondrosarcoma, 4 synovial sarcoma, and 3 rhabdomyosarcoma, which were obtained at initial surgery at the department of orthopaedic surgery at Mie University Hospital, were examined by reverse transcription (RT)-PCR. Schwannoma, desmoid and lipoma samples were used as controls. Tissue samples for immunohistochemical staining were obtained from 25 EWS patients who underwent an open biopsy or a surgical resection. For enzyme-linked immunosorbent assay (ELISA), we used serum samples of 3 osteosarcomas, 1 osteofibrous dysplasia, 1 chondrosarcoma, 1 synovial sarcoma, 6 EWS and 4 healthy volunteers. Basically sera were isolated before the chemotherapy except for few cases. Informed consent was obtained from each patient or parent and volunteer. This study was approved by the ethics committee at Mie University.

Antibodies and other reagents. A rabbit polyclonal anti-ADAMTS4 antibody which was raised against amino acids 764-837 of human ADAMTS4 (Santa Cruz Biotechnology, Santa Cruz, CA, USA) and a horseradish peroxidase (HRP)-conjugated goat anti-rabbit IgG secondary antibody (Bio-Rad Laboratories, Hercules, CA, USA) were used for immunoprecipitation (IP)-Western blot analysis. Immunostaining was performed by using the following antibodies: the same anti-ADAMTS4 antibody as used for IP-Western analysis, an N-universal rabbit IgG (Dako, Kyoto, Japan), an HRP-conjugated anti-rabbit IgG antibody (Nichirei Biosciences, Tokyo, Japan) for immunohistochemistry, and an Alexa488-conjugated anti-rabbit IgG antibody (Invitrogen, Carlsbad, CA, USA) for immunofluorescence microscopy. For ELISA, a monoclonal anti-ADAMTS4 antibody raised against amino acids 213-685 of the recombinant human ADAMTS4 (R&D Systems), a biotinylated goat anti-ADAMTS4 antibody raised against amino acids 213-685 of the recombinant human ADAMTS4 and an Avidin-HRP (eBioscience, San Diego, CA, USA) were used.

Screening of EWS cDNA library by SST. A human EWS cDNA library was screened by SST-REX as previously described (24,25). Briefly, poly(A)$^+$ RNA was prepared from EWS cell lines using the FastTrack2.0 Kit (Invitrogen). The cDNA was synthesized from the mixture of poly(A)$^+$ RNAs of 6 EWS cell lines with random hexamers, using the SuperScript Choice System (Invitrogen) according to the manufacturer's instructions. The synthesized cDNA was size-separated by electrophoresis on an agarose gel. Fractions greater than 500 bp were collected and inserted into *Bst*XI sites of pMX-SST (25) using *Bst*XI adaptors (Invitrogen). Ba/F3 cells were infected with the retroviruses expressing the EWS-derived cDNA library and selected for growth in the absence of IL-3. Genomic DNAs extracted from IL-3-independent clones were subjected to PCR to recover the

Table I. Primer sequences used in RT-PCR analyses in murine tissues.

Gene	Sense	Antisense
DKFZP564O0823	5'-CCATTGCCTGTCTCTCTCATGACA-3'	5'-GAGCTGTGCTCTTCTGTTGGTGA-3'
ADAMTS4	5'-GAGCTGTGCTCTTCTGTTGGTGA-3'	5'-CAGAGAAGCGAAGCGCTTGGTT-3'
DNER	5'-GACATAATCCTGCCCCGCTCT-3'	5'-CTCTGATGGCTTCGTGGCACAT-3'
NGFR	5'-CGTGTTCTCCTGCCAGGACAA-3'	5'-GCTGTGCAGTTTCTCTCCCTCT-3'
LRRN6A	5'-GTCTTCACCCGGCCTCAGCAA-3'	5'-CCCTCGATTGTACCGATTGGGTT-3'
ECSM2	5'-GACAACTCAGACCTCGCAGGAA-3'	5'-CATTGGCTGTGGAGCAGCTTTCA-3'
LGALS3BP	5'-CAGGACTACTGTGGACGGCTT-3'	5'-CTACTCCAGGTGGAAGAGGTGTA-3'
PTPRF	5'-GCTGGCCCAGGAGAAGAGTT-3'	5'-GCTCTGCCCATTGTACAGGATCTT-3'
FCGRT	5'-GCTGTGAACTGGCCTCGGATA-3'	5'-CCAGCAATGACCATGCGTGGAA-3'
LAMP2	5'-CGCTGTCTCTTGGGCTGTGAAT-3'	5'-GGCACCTTCTCCTCAGTGATGTT-3'
RCN1	5'-CTAAGCCCCGGACGAGAGCAA-3'	5'-GGCCATTGTCCTCGTGGGAA-3'
MMP14	5'-CATGAGTTGGGGCATGCCCTA-3'	5'-CGGCCAAGCTCCTTAATGTGCTT-3'
SDC2	5'-CTCCATTGAGGAAGCTTCAGGAGT-3'	5'-CTTCTGGTAAGCTGCGCTGGAT-3'
DAG1	5'-GGAAGCCCACGGTCACCATT-3'	5'-GCTTGAGCTTGTCGGTAGTGGTA-3'
EPCR	5'-GGCAACGCCTCTCTGGGAAAA-3'	5'-CGGCCACACCAGCGATTATGAA-3'
CD97	5'-CTGGAACAAAGCCTTCGGACCTT-3'	5'-GTCGGTGTCCCAGTACCCATT-3'
CD99L2	5'-GTCCAGAGAGGATATGGAGACACA-3'	5'-GGTTCTGCAGACTGCGTTTCTTG-3'
IGFBP5	5'-GCGACGAGAAAGCTCTGTCCAT-3'	5'-GCCTTGTTCGGATTCCTGTCTCA-3'
CLU	5'-GAAGGCATTCCCCGGAAGTGTGTA-3'	5'-GCTGGACATCCATGGCCTGTT-3'
LSAMP	5'-GCTCTGGAATACAGCCTCCGAA-3'	5'-GTGTCATCCCCGGTACCACTCAA-3'
NPTN	5'-GTAACCTCACTTCCAGCTCTCACA-3'	5'-GGAGGCAGAGCCAATGGAGTT-3'
EFNA5	5'-GCAGCAACCCCAGATTCCAGA-3'	5'-GATGGCTCGGCTGACTCATGTA-3'
PODXL	5'-CCTTCACCAGTAGCAGTGGACAA-3'	5'-CCACTGTAGACGCCATAGACTGT-3'
TMEM123	5'-CCACTCAGTGCTGACCTCCAA-3'	5'-GTTCGTCAATGCTTCGGTACCGAA-3'
GAPDH	5'-CAGTATGACTCCACTCACGGCAA-3'	5'-CAGATCCACGACGGACACATTG-3'

integrated cDNAs using vector primers. The resulting PCR fragments were sequenced and analyzed.

RT-PCR analysis. RT-PCR was carried out to detect *ADAMTS4* transcript in tumor cell lines, murine tissues and patients' samples. Total RNA was isolated with acid guanidium-phenol-chloroform method, and then 5 μg RNA was reverse-transcribed to cDNA in a total volume of 33 μl with random hexamers by using the Ready-To-Go You-Prime First-Strand Beads (GE Healthcare UK, Buckinghamshire, UK). RT-PCR was performed with the programmable cyclic reactor under the following conditions: denaturation at 94˚C for 3 min followed by 30 cycles of amplification (94˚C for 30 sec, 60˚C for 30 sec, and 72˚C for 45 sec). PCR product was separated by 1-2% agarose gel electrophoresis and visualized by ethidium bromide staining. The primers used for RT-PCR was described in Tables I and II.

Cloning of the full-length cDNA encoding ADAMTS4. Full-length *ADAMTS4* was generated as follows. The first half of *ADAMTS4* (1-1194 bp) was isolated from pMX-SST vector by digestion with *Bam*HI. Based on the sequence data, the last half (1195-2514 bp) were amplified by PCR from cDNAs of the EWS cell line SJES-5, and digested with *Bam*HI and *Not*I. The fragment was subcloned into a pMXs-puro retroviral vector (37). The resultant vector was digested with *Bam*HI, and then ligated with the *Bam*HI fragment of the first half of *ADAMTS4*. The primers used for amplification are as follows: SST5', 5'-GGGGGTGGACCATCCTCTA-3'; SST3', 5'-CGCGCAGCTGTAAACGGTAG-3'; ADAMTS4-FL-S, 5'-GAAAGAATTCGCTGCAGTACCAGTGCCATG-3'; ADAMTS4-FL-S2, 5'-GAGCACCTCTCGCCATGTCA-3'; ADAMTS4-FL-AS, 5'-GAAAGAGAATTCGCGGCC GCTTATTTCCTGCCCGCCCAGG-3'; ADAMTS4-AS2, 5'-CTTTGGATCCACATGAGCCATCACAGGGGCCA TGACATGGCGAGAGGTGCTCAAAGCCCATTCAAA CTGATGCATG-3'.

Transfection and infection. Retroviral transfection was done as described previously (36,37). Briefly, retroviruses were generated by transient transfection of Plat-E packaging cells (36) with FuGENE 6 (Roche Diagnostics, Basel, Switzerland). Ba/F3 and NIH3T3 cells were infected with the retroviruses in the presence of 10 μg/ml polybrene. Selection with G418 or puromycin was started 48 h after infection.

Small interfering (si)RNA design and transfection experiments. EWS-FLI1 specific siRNA (siEF1) for SJES-5 cell line was designed as previously described (38). As a negative control, siGFP was employed (Hayashi-Kasei, Osaka, Japan).